

Fast method for quantum mechanical molecular dynamics

Anders M. N. Niklasson* and Marc J. Cawkwell

Theoretical Division, Los Alamos National Laboratory, Los Alamos, New Mexico 87545

(Dated: May 26, 2022)

As the processing power available for scientific computing grows, first principles Born-Oppenheimer molecular dynamics simulations are becoming increasingly popular for the study of a wide range of problems in materials science, chemistry and biology. Nevertheless, the computational cost of Born-Oppenheimer molecular dynamics still remains prohibitively large for many potential applications. Here we show how to avoid a major computational bottleneck: the self-consistent-field optimization prior to the force calculations. The optimization-free quantum mechanical molecular dynamics method gives trajectories that are almost indistinguishable from an “exact” microcanonical Born-Oppenheimer molecular dynamics simulation even when low pre-factor linear scaling sparse matrix algebra is used. Our findings show that the computational gap between classical and quantum mechanical molecular dynamics simulations can be significantly reduced.

I. INTRODUCTION

The past three decades have witnessed a dramatic increase in the use of the molecular dynamics simulation method [1, 2]. While it is unquestionably a powerful and widely used tool, its ability to calculate physical properties is limited by the quality and the computational complexity of the interatomic potentials. Among computationally tractable models, the most accurate are explicitly quantum mechanical with interatomic forces calculated on-the-fly using a nuclear potential energy surface that is determined by the electronic ground state within the Born-Oppenheimer approximation [2–4]. In Hartree-Fock [5, 6] or density functional theory [7–10], the electronic ground-state density is given through a self-consistent-field (SCF) optimization procedure, which involves iterative mixed solutions of the single-particle eigenvalue equations and accounts for details in the charge distribution. Since the interatomic forces are sensitive to the electrostatic potential [11], molecular dynamics simulations are often of poor quality without a high degree of self-consistent-field convergence. This is unfortunate since the iterative self-consistent-field procedure is computationally expensive and in practice always approximate.

Recently there have been efforts to reduce the computational cost of the self-consistent-field optimization without causing any significant deviation from “exact” Born-Oppenheimer molecular dynamics simulations [12–14]. In this article we go one step further, and in analogy to time-dependent techniques such as Ehrenfest molecular dynamics [15–17] or the Car-Parrinello method [2, 18–23], we show how the electronic ground state optimization can be circumvented fully without any noticeable reduction in accuracy in comparison to “exact” Born-Oppenheimer molecular dynamics.

Our optimization-free dynamics is based on a reformulation of extended Lagrangian Born-Oppenheimer

molecular dynamics [35] in the limit of vanishing self-consistent-field optimization. The method is presented within a general free energy formulation that is valid also at finite electronic temperatures and should be applicable to a broad class of materials. In addition to the removal of the costly self-consistent-field optimization we also demonstrate compatibility with low pre-factor linear scaling electronic structure theory [24–26]. The combined scheme provides a very efficient, energy conserving, low-complexity method for performing accurate quantum molecular dynamics simulations.

II. FAST QUANTUM MECHANICAL MOLECULAR DYNAMICS

A. Born-Oppenheimer molecular dynamics

Born-Oppenheimer molecular dynamics based on density functional theory can be described by the Lagrangian

$$\mathcal{L}^{\text{BO}}(\mathbf{R}, \dot{\mathbf{R}}) = \frac{1}{2} \sum_k M_k \dot{R}_k^2 - U[\mathbf{R}; \rho], \quad (1)$$

where the potential energy,

$$U[\mathbf{R}; \rho] = 2 \sum_{i \in \text{occ}} \varepsilon_i - \frac{1}{2} \iint \frac{\rho(\mathbf{r})\rho(\mathbf{r}')}{|\mathbf{r}' - \mathbf{r}|} d\mathbf{r}' d\mathbf{r} - \int V_{\text{xc}}[\rho]\rho(\mathbf{r})d\mathbf{r} + E_{\text{xc}}[\rho] + E_{\text{zz}}[\mathbf{R}], \quad (2)$$

is calculated at the self-consistent electronic ground state density, $\rho(\mathbf{r})$, for the nuclear configuration $\mathbf{R} = \{R_k\}$ [9, 10]. Here, ε_i are the (doubly) occupied eigenvalues of the effective single-particle Kohn-Sham Hamiltonian,

$$H[\rho] = -\frac{1}{2}\nabla^2 + V_{\text{n}}(\mathbf{R}, \mathbf{r}) + \int \frac{\rho(\mathbf{r}')}{|\mathbf{r}' - \mathbf{r}|} d\mathbf{r}' + V_{\text{xc}}[\rho], \quad (3)$$

where $V_{\text{xc}}[\rho]$ is the exchange correlation potential, $V_{\text{n}}(\mathbf{R}, \mathbf{r})$ the external (nuclear) potential, and $-\frac{1}{2}\nabla^2$ the kinetic energy operator. $E_{\text{zz}}[\mathbf{R}]$ is the electrostatic ion-ion repulsion and $E_{\text{xc}}[\rho]$ the exchange correlation energy.

*Corresponding Author Email: amn@lanl.gov

If the electron density deviates from the ground state density ρ by some small amount $\delta\rho$, the error in the potential energy is essentially of the order $\delta\rho^2$, depending on the particular formulation used for calculating $U[\mathbf{R}; \rho + \delta\rho]$ [33, 34, 47]. However, since the Hellmann-Feynman theorem is valid only at the ground state density, we do not have a simple expression for the forces that avoids calculating derivatives of the electronic density, $\partial(\rho + \delta\rho)/\partial R_k$. In practical calculations, the accuracy of the potential energy can therefore not be expected to hold also for the forces and a high degree of self-consistent-field convergence is therefore typically required.

B. Extended Lagrangian molecular dynamics

Here we outline how we can circumvent the self-consistent-field procedure in Born-Oppenheimer molecular dynamics. Instead of recalculating the ground state density before each force evaluation with an iterative optimization procedure, the idea here is to use an auxiliary density $n(\mathbf{r})$, as in extended Lagrangian Born-Oppenheimer molecular dynamics [35–39], which evolves through a harmonic oscillator centered around the ground state density $\rho(\mathbf{r})$. Based on a general free energy formulation of extended Lagrangian Born-Oppenheimer molecular dynamics [39] in the limit of vanishing self-consistent-field optimization, we define the extended Lagrangian:

$$\begin{aligned} \mathcal{L}(\mathbf{R}, \dot{\mathbf{R}}, n, \dot{n}) &= \frac{1}{2} \sum_k M_k \dot{R}_k^2 - \mathcal{U}[\mathbf{R}; n] + T_e \mathcal{S}[\mathbf{R}; n] \\ &+ \frac{1}{2} \mu \int \dot{n}(\mathbf{r})^2 d\mathbf{r} - \frac{1}{2} \mu \omega^2 \int (\rho(\mathbf{r}) - n(\mathbf{r}))^2 d\mathbf{r}. \end{aligned} \quad (4)$$

While the potential and entropy terms, \mathcal{U} and \mathcal{S} , are well defined at the ground state density [9], i.e. when $n = \rho$, there are several different options when n deviates from ρ , e.g. the Harris-Foulkes functional [33, 34, 47]. In a more general case, the potential energy and entropy term may therefore also be determined by $n(\mathbf{r})$ implicitly through an additional function $\sigma[n(\mathbf{r})]$, i.e. $\mathcal{U}[\mathbf{R}; n] \equiv \mathcal{U}[\mathbf{R}; n, \sigma[n]]$ and $\mathcal{S}[\mathbf{R}; n] \equiv \mathcal{S}[\mathbf{R}; n, \sigma[n]]$. Here $\sigma[n(\mathbf{r})]$ is a temperature dependent density given from the diagonal part of the real-space representation of the (doubly occupied) density matrix, which is given through a Fermi-operator expansion [9] of the effective single-particle Hamiltonian, $H[n]$, i.e.

$$\sigma(\mathbf{r}) \equiv \sigma[n(\mathbf{r})] = 2 \left(e^{\beta(H[n] - \mu_0 I)} + 1 \right)^{-1} \Big|_{\mathbf{r}=\mathbf{r}'}. \quad (5)$$

At zero electronic temperature the Fermi-operator expansion corresponds to a step function with the step formed at the chemical potential, μ_0 . In our Lagrangian above, μ and ω are fictitious mass and frequency parameters of the harmonic oscillator and β is the inverse

electronic temperature, i. e. $\beta = 1/(k_B T_e)$. The purpose of the entropy-like term $\mathcal{S}[\mathbf{R}; n]$ is here to make the derived forces of our dynamics variationally correct for a given entropy-independent density, $n(\mathbf{r})$, at any electronic temperature. This approach is different from the regular formulation where the density is determined by the entropy through the minimization of the electronic free energy functional [9, 40–42].

1. Equations of motion

The molecular trajectories corresponding to the extended free energy Lagrangian \mathcal{L} in Eq. (4) are determined by the Euler-Lagrange equations of motion,

$$\begin{aligned} M_k \ddot{R}_k &= - \left. \frac{\partial \mathcal{U}[\mathbf{R}; n]}{\partial R_k} \right|_n + T_e \left. \frac{\partial \mathcal{S}[\mathbf{R}; n]}{\partial R_k} \right|_n \\ &- \frac{\mu \omega^2}{2} \left. \frac{\partial}{\partial R_k} \int (\rho(\mathbf{r}) - n(\mathbf{r}))^2 d\mathbf{r} \right|_n, \end{aligned} \quad (6)$$

and

$$\begin{aligned} \mu \ddot{n}(\mathbf{r}) &= \mu \omega^2 (\rho(\mathbf{r}) - n(\mathbf{r})) \\ &- \left. \frac{\delta \mathcal{U}[\mathbf{R}; n]}{\delta n} \right|_{\mathbf{R}} + T_e \left. \frac{\delta \mathcal{S}[\mathbf{R}; n]}{\delta n} \right|_{\mathbf{R}}, \end{aligned} \quad (7)$$

where the partial derivatives are taken with respect to constant density, n , or coordinates, \mathbf{R} . The limit $\mu \rightarrow 0$ gives us the equations of motion of our extended Lagrangian dynamics,

$$M_k \ddot{R}_k = - \left. \frac{\partial \mathcal{U}[\mathbf{R}; n]}{\partial R_k} \right|_n + T_e \left. \frac{\partial \mathcal{S}[\mathbf{R}; n]}{\partial R_k} \right|_n \quad (8)$$

$$\ddot{n}(\mathbf{r}) = \omega^2 (\rho(\mathbf{r}) - n(\mathbf{r})), \quad (9)$$

where we have defined $\mathcal{S}[\mathbf{R}; n]$ such that

$$\left. \frac{\delta \mathcal{U}[\mathbf{R}; n]}{\delta n} \right|_{\mathbf{R}} = T_e \left. \frac{\delta \mathcal{S}[\mathbf{R}; n]}{\delta n} \right|_{\mathbf{R}}. \quad (10)$$

As is shown in the Appendix (Sec. VII A), the corresponding property for $\partial \mathcal{S} / \partial R_k$ is also of importance for the calculation of the Pulay force in Eq. (8). Notice that these equations still require a full self-consistent field optimization, since the auxiliary density $n(\mathbf{r})$ evolves around the ground state density $\rho(\mathbf{r})$.

Since the nuclear degrees of freedom do not depend on the mass parameter μ in Eqs. (8) and (9), the total free energy,

$$E_{\text{tot}} = \frac{1}{2} \sum_k M_k \dot{R}_k^2 + \mathcal{U}[\mathbf{R}; n] - T_e \mathcal{S}[\mathbf{R}; n], \quad (11)$$

is a constant of motion in the limit of vanishing μ . Moreover, if E_{tot} is close to the exact ground state free energy

for approximate densities $n(\mathbf{r})$, we can also expect that the forces of the extended Lagrangian dynamics should be accurate.

The forces in Eq. (8) are calculated at the approximate, unrelaxed, density $n(\mathbf{r})$ using a Hellmann-Feynman-like expression, where the partial derivatives are taken with respect to a constant density $n(\mathbf{r})$. This is possible only because $n(\mathbf{r})$ appears as an independent dynamical variable. In general, as mentioned above, this can not be assumed, since the Hellmann-Feynman force expression is formally applicable only at the ground density. A more detailed derivation of explicit force expressions is given in the Appendix.

2. Entropy contribution

Depending on the particular functional form chosen for the potential energy term, $\mathcal{U}(\mathbf{R}; n)$, we may not have access to a simple explicit expression of $\mathcal{S}[\mathbf{R}; n]$ that fulfills Eq. (10). In this case an approximate entropy term has to be used. This has no effect on the dynamics in Eqs. (8) and (9), since the forces remain exact by definition. An approximation of the entropy term therefore only affects the estimate of the constant of motion, E_{tot} , in Eq. (11).

We have found that the regular expression for the electronic entropy [9],

$$\mathcal{S}[\mathbf{R}; n] = -2k_{\text{B}} \sum_i \{f_i \ln(f_i) + (1 - f_i) \ln(1 - f_i)\}, \quad (12)$$

which formally is defined only at the ground state density, i.e. when $n = \rho$, typically provides a highly accurate approximation also for approximate densities as will be illustrated in the examples below. Here f_i are the occupation numbers of the states, i.e. the eigenvalues of the density matrix in Eq. (5). These are determined by the Fermi-Dirac distribution of the single-particle eigenvalues ε_i of the Hamiltonian $H[n]$, i.e.

$$f_i = \left[e^{\beta(\varepsilon_i - \mu)} + 1 \right]^{-1}. \quad (13)$$

By comparing the calculation of E_{tot} in Eq. (11) using the approximate entropy term, $\mathcal{S}[\mathbf{R}; n]$, in Eq. (12) to “exact”, fully optimized, Born-Oppenheimer molecular simulations, we can estimate the accuracy of our dynamics.

C. Fast quantum mechanical molecular dynamics

As in extended Lagrangian Born-Oppenheimer molecular dynamics, the irreversibility of regular Born-Oppenheimer molecular dynamics that is caused by the self-consistent-field optimization, can be avoided, since the density $n(\mathbf{r})$ can be integrated using a reversible geometric integration algorithm [35, 36, 44, 45], e.g. the Verlet algorithm as in Eq. (16) below. This prevents the

unphysical drift in the energy and phase space of regular Born-Oppenheimer molecular dynamics [12–14] and our dynamics will therefore exhibit long-term stability of the free energy E_{tot} in Eq. (11).

A main problem so far is that we still need to calculate the self-consistent ground state density $\rho(\mathbf{r})$ in the integration of $n(\mathbf{r})$ in Eq. (9). Fortunately, various geometric integrations of the auxiliary density $n(\mathbf{r})$ in Eq. (9) are stable also for approximate ground state density estimates of $\rho(\mathbf{r})$, as long as the approximation of $\rho(\mathbf{r})$ is at least infinitesimally closer to the exact ground state compared to $n(\mathbf{r})$. Using an integration time step of δt , this stability holds if the value of the dimensionless variable $\kappa = \delta t^2 \omega^2$ is chosen to be appropriately small [36, 45, 46]. For energy functionals that are convex in the vicinity of the ground state density we may therefore replace $\rho(\mathbf{r})$ in Eq. (9) by a linear combination $(1 - c)n + c\sigma$ [43], which gives us the approximate equations of motion

$$M_k \ddot{R}_k = - \left. \frac{\partial \mathcal{U}[\mathbf{R}; n]}{\partial R_k} \right|_n + T_e \left. \frac{\partial \mathcal{S}[\mathbf{R}; n]}{\partial R_k} \right|_n, \quad (14)$$

and

$$\ddot{n}(\mathbf{r}) = \omega^2 (\sigma(\mathbf{r}) - n(\mathbf{r})), \quad (15)$$

where the constant ω^2 has been rescaled by c . The Verlet integration of Eq. (15), including a weak dissipation to avoid an accumulation of numerical noise [36, 37],

$$n_{t+\delta t} = 2n_t - n_{t-\delta t} + \delta t^2 \omega^2 (\sigma_t - n_t) + \alpha \sum_{k=0}^K c_k n_{t-k\delta t}, \quad (16)$$

is therefore stable if a sufficiently small positive value of $\kappa = \delta t^2 \omega^2$ is chosen [36]. Thus, without any self-consistent-field optimization of $\rho(\mathbf{r})$, the previously optimized values of κ in Ref. [36, 45, 46] should be rescaled by a positive factor ≤ 1 . Certain ill behaved (non-convex) functionals with self-consistent-field instabilities [43] can not be treated in this framework.

The proposed molecular dynamics as given by Eqs. (14) and (15) is the central result of this paper. The equations of motion do not involve any ground state self-consistent-field optimization prior to the force evaluations and only one single diagonalization or density matrix construction is required in each time step. The frequency ω of the electronic density is well separated from the nuclear vibrational oscillations. Using a value of $\delta t \omega = \sqrt{\kappa} \approx 1$ and an integration time step δt , which is $\sim 1/15$ of the period of the nuclear motion, the frequencies differ by a factor of 5. As will be demonstrated in the examples below, the scheme is also fully compatible with linear scaling electronic structure theory [24, 25]. This compatibility is crucial in order to simulate large systems. The removal of the costly ground state optimization, in combination with low-complexity linear scaling solvers, provide a computationally fast quantum mechanical molecular dynamics (Fast-QMMD) that can match

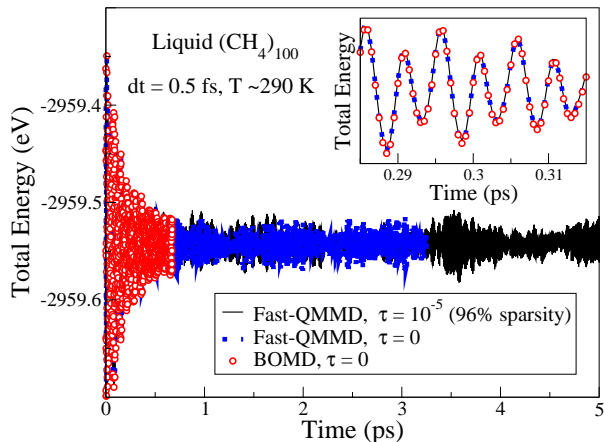


FIG. 1: Total energy fluctuations, Eq. (11), using “exact” (4 SCF/step) Born-Oppenheimer molecular dynamics (BOMD), and the fast quantum mechanical molecular dynamics, Eqs. (14) and (15), (Fast-QMMD), with ($\tau > 0$) or without ($\tau = 0$) thresholding applied in the low pre-factor linear scaling solver [26]. The simulations were performed with the molecular dynamics program LATTE using self-consistent-charge density functional based tight-binding theory in an orthogonal formulation at $T_e = 0$, i.e. as in Eqs. (57), (58) and (60).

the fidelity and accuracy of regular Born-Oppenheimer molecular dynamics.

There are several alternative approaches to derive or motivate the equations of motion of the fast quantum mechanical molecular dynamics, Eqs. (14) and (15), and details of the dynamics may vary depending on the choice of the functional form of $\mathcal{U}(\mathbf{R}; n)$. However, the particular derivation presented here is the most transparent and general approach that we have found so far.

The equations of motion are given in terms of the electron density, but they should be generally applicable to a large class of methods, such as Hartree-Fock theory, which is analyzed in the Appendix (Sec. VII A), or plane wave pseudo-potential methods [37]. Here we will demonstrate our fast quantum mechanical molecular dynamics scheme using self-consistent-charge density functional tight-binding theory [47–50], as implemented in the electronic structure code LATTE [51], either with an orthogonal or a non-orthogonal representation and both at zero and at finite electronic temperatures. With this method we can easily reach the time and length scales necessary to establish long-term energy conservation and linear scaling of the computational cost. Details of the computational method and our particular choices of $\mathcal{U}(\mathbf{R}; n)$ are given in the Appendix.

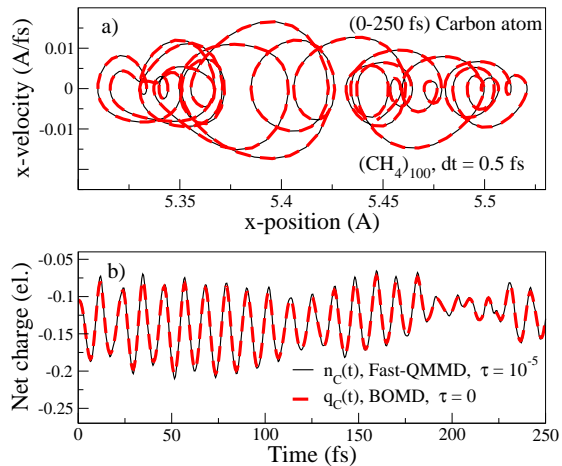


FIG. 2: Panel a) shows the x-plane phase space trajectory of a single carbon atom (C) based on an “exact” (4 SCF/step) Born-Oppenheimer molecular dynamics (BOMD, dashed line) and the fast quantum mechanical molecular dynamics (Fast-QMMD, solid line). Panel b) shows the fluctuations in the net auxiliary charge $n_i(t)$ and ground state charge $q_i(t)$ for the same carbon atom ($i=C$). The numerical threshold τ is applied in the linear scaling solver [26]. The simulations were performed with the program LATTE using self-consistent-charge tight-binding theory in an orthogonal formulation at zero electronic temperature, i.e. as in Eqs. (57), (58) and (60).

TABLE I: Wall clock timings of the fast quantum mechanical molecular dynamics (Fast-QMMD) simulations in comparison to Born-Oppenheimer molecular dynamics (BOMD) (4 SCF/step), without ($\tau = 0$) and with ($\tau > 0$) a low pre-factor linear scaling solver for the density matrix [26] with threshold tolerance τ . The program (LATTE in its orthogonal formulation at $T_e = 0$) was executed on a single core of a 2.66 GHz Quad-Core Intel Xeon processor.

Polyethene chain $C_{100}H_{202}$	Efficiency
BOMD ($\tau = 0$)	7.5 s/step
Fast-QMMD ($\tau = 0$)	1.5 s/step
Fast-QMMD ($\tau = 10^{-5}$)	0.61 s/step
Liquid Methane $(CH_4)_{100}$	Efficiency
BOMD ($\tau = 0$)	12.5 s/step
Fast-QMMD ($\tau = 0$)	2.5 s/step
Fast-QMMD ($\tau = 10^{-5}$)	0.35 s/step

III. EXAMPLES

A. Orthogonal representation

Figure 1 shows the fluctuations in the total energy (kinetic plus potential) using the fast quantum mechanical molecular dynamics, Eqs. (14) and (15), as implemented in Eqs. (57), (58) and (60), and an “exact” Born-Oppenheimer molecular dynamics [35], for liquid methane (density = 0.422 g/cm^3) at room temperature.

The calculations were performed with the LATTE molecular dynamics program using periodic boundary conditions and an integration time step of $\delta t = 0.5$ fs. Since the molecular system is chaotic, any infinitesimally small deviation will eventually lead to a divergence between different simulations. However, even after hundreds of time steps and over 300 fs of simulation time the total energy curves are virtually on top of each other as is seen in the inset. The same remarkable agreement is seen in Fig. 2, which shows the projected phase space of an individual carbon atom and the fluctuations of its net charge. In this case the C atom was displaced compared to the simulation in Fig. 1 to further enhance the charge fluctuations.

B. Linear scaling

The fast quantum mechanical molecular dynamics scheme is also stable in combination with approximate linear scaling sparse matrix algebra [24, 25]. Using the recursive second order spectral projection method for the construction of the density matrix [26] with a numerical threshold, $\tau = 10^{-5}$, below which all elements are set to zero after each individual projection, we notice excellent accuracy and stability in Fig. 1 without any systematic drift in the total energy.

Despite their high efficiency and low computational pre-factor compared to alternative linear scaling electronic structure methods [52], it has been argued that recursive purification algorithms are non-variational and therefore incompatible with forces of a conservative system [25], which is necessary for long-term energy conservation. As is evident from Figs. 1 and 2, this is not a problem. The graphs are practically indistinguishable from “exact” Born-Oppenheimer molecular dynamics, without any signs of a systematic drift in the total energy. The corresponding linear scaling compatibility with microcanonical simulations was recently also demonstrated for self-consistent-field-optimized extended Lagrangian Born-Oppenheimer molecular dynamics [27].

The gain in speed using the fast quantum mechanical molecular dynamics scheme in comparison to Born-Oppenheimer molecular dynamics is illustrated by the wall-clock timings shown in Tab. I.

C. Non-orthogonal representation

For non-orthogonal representations at finite electronic temperatures, a Pulay force term and a finite approximate entropy contribution to the total free energy have to be included. Figures 3 and 4 illustrate the total energy fluctuations for the fast quantum mechanical molecular dynamics simulations of a hydrocarbon chain as implemented in LATTE using Eqs. (50), (51) and (55), with the approximate entropy term in Eq. (56). The electronic temperature of the examples in Figure 3 is set

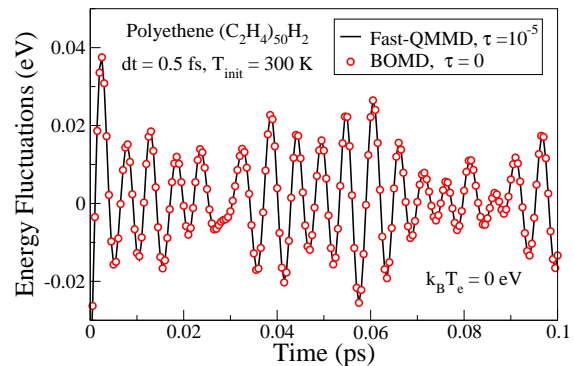


FIG. 3: Total energy fluctuations, Eq. (11), using “exact” (4 SCF/step) Born-Oppenheimer molecular dynamics (BOMD), and the fast quantum mechanical molecular dynamics, Eqs. (14) and 15), (Fast-QMMD), with ($\tau = 10^{-5}$) or without ($\tau = 0$) thresholding applied in the low pre-factor linear scaling solver [26]. The simulations were performed with the molecular dynamics program LATTE in the non-orthogonal formulation at $k_B T_e = 0$ eV, i.e. as implemented in Eqs. (50), (51) and (55) with the entropy term approximated by $\mathcal{S} = 0$.

to zero, $k_B T_e = 0$ eV, and for the examples in Fig. 4, $k_B T_e = 2$ eV. In the first time step the initial nuclear temperature, T_{init} , was set to 300 K using a Gaussian distribution of the velocities. Despite the approximation of ρ in Eq. (15) and the approximate estimate of the entropy contribution to the free energy there is virtually no difference seen between the fast quantum mechanical and the Born-Oppenheimer molecular dynamics simulations.

As in the orthogonal case, the non-orthogonal formulation of our fast quantum mechanical molecular dynamics is fully compatible with linear scaling complexity in the construction of the density matrix at $T_e = 0$ K. In Fig. 3 the reduced complexity simulation shows no significant deviation from “exact” Born-Oppenheimer molecular dynamics. At finite electronic temperatures, the linear scaling construction of the Fermi operator [28, 42] has not yet been implemented.

D. Long-term stability and conservation of the total energy

To assess the long-term energy conservation and the stability we use a test system comprised of 16 molecules of isocyanic acid, HNCO, at a density of 1.14 g cm^{-3} . The system was first thermalized to a temperature of 300 K over a simulation time of 12.5 ps by the rescaling of the nuclear velocities. The simulations used an integration time step, δt , of 0.25 ps. The simulations were performed using self-consistent tight-binding the-

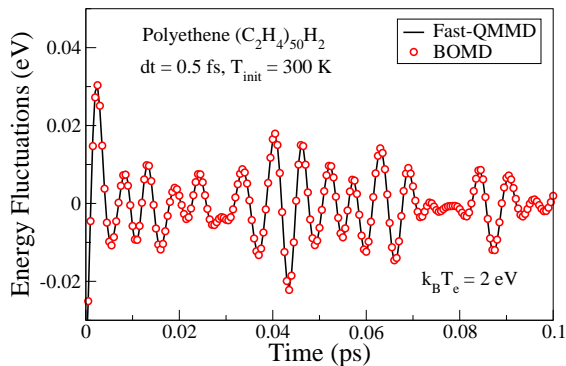


FIG. 4: Total free energy fluctuations, Eq. (11), using “exact” (4 SCF/step) Born-Oppenheimer molecular dynamics (BOMD), and the fast quantum mechanical molecular dynamics, Eqs. (14) and (15), (Fast-QMMD). The simulations were performed with the molecular dynamics program LATTE using the non-orthogonal formulation at an electronic temperature of $k_B T_e = 0.5$ eV, i.e. as implemented in Eqs. (50), (51) and (55) with the entropy term approximated by Eq. (56).

ory [47–50] with a non-orthogonal basis as implemented in LATTE, using Eqs. (50), (51) and (55) with the entropy term approximated by Eq. (56).

Fast quantum mechanical molecular dynamics and “exact” Born-Oppenheimer molecular dynamics simulations with 4 self-consistent field cycles per time step were performed over 250,000 time steps (62.5 ps) with $T_e = 0$ K and $k_B T_e = 0.5$ eV. The latter temperature is small with respect to the HOMO-LUMO gap of HNCO, which is about 6.0 eV, yet the entropy term, Eq. (12) or Eq. (56), contributes about 0.19 eV to the total energy owing to the partial occupation of states in the vicinity of the chemical potential. Trajectories computed at $T_e = 0$ K with “exact” Born-Oppenheimer molecular dynamics and the fast quantum mechanical molecular dynamics method without ($\tau = 0$) and with ($\tau = 10^{-5}$) linear scaling constructions of the density matrix are presented in Fig. 5. The standard deviation of the fluctuations of the total energy about its mean and an estimate of the level of the systematic drift of the total energies are presented in Table II. These data show that the fast quantum mechanical molecular dynamics simulations yield trajectories that are effectively indistinguishable from the “exact” Born-Oppenheimer trajectories. Moreover, as was seen above, the fast quantum mechanical molecular dynamics scheme appears to be fully compatible with linear scaling construction of the density matrix and the resulting approximate forces, since this trajectory differs from the “exact” Born-Oppenheimer molecular dynamics trajectory only by a small-amplitude random-walk of the total energy about its mean [27]. The systematic drift

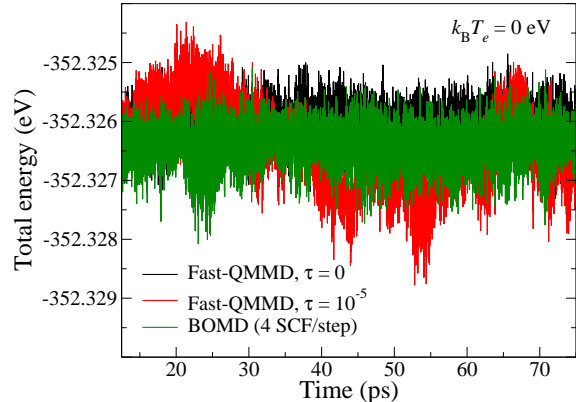


FIG. 5: Total energy versus time for liquid isocyanic acid with a nuclear temperature of 300 K and $T_e = 0$ K computed with “exact” Born-Oppenheimer MD and the Fast QMMD method with exact and approximate linear scaling density matrix constructions. The numerical threshold τ is applied in the linear scaling solver [26] below which all matrix elements are set to zero after each iteration.

in energy is several orders of magnitude smaller than in previous attempts to combine linear scaling solvers with regular Born-Oppenheimer molecular dynamics [29–32].

The trajectories computed with an electronic temperature corresponding to $k_B T_e = 0.5$ eV differ qualitatively from those computed with zero electronic temperature. Figure 6 and Table II show that while the “exact” Born-Oppenheimer trajectory conserves the free energy to an extremely high tolerance over the duration of the simulation, the total free energy in the fast quantum mechanical molecular dynamics simulation exhibit random-walk behaviour about the mean value. Although the fast quantum mechanical molecular dynamics simulations involve an approximate expression for the entropy, we find that this alone cannot account for the level of fluctuations observed. Instead, we have found that the rescaling of the κ value in the integration, Eq. (16), affects this random-walk. By changing the rescaling factor to 3/4, instead of 1/2 as in all the other examples, the amplitude of the random walk is significantly reduced. Nevertheless, the fast quantum mechanical molecular dynamics trajectories at finite electronic temperature exhibit systematic drifts in the total energy that are negligible and the fluctuations of the total energy about the mean are of the same order as those that arise from the application of the approximate linear scaling method at $T_e = 0$ K.

IV. CONVERGENCE PROPERTIES

The fast quantum mechanical molecular dynamics scheme, Eqs. (14) and (15), can also be analyzed in

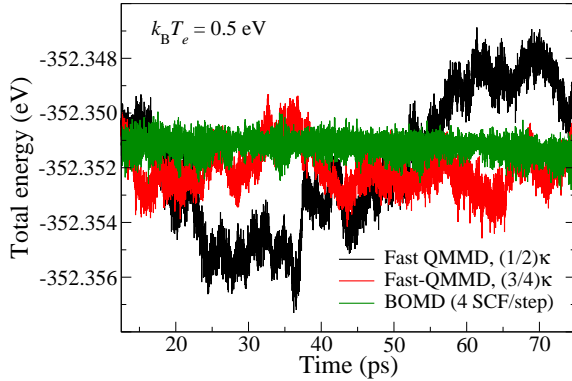


FIG. 6: Total free energy versus time for liquid isocyanic acid with a nuclear temperature of 300 K and $k_B T_e = 0.5$ eV computed with “exact” Born-Oppenheimer molecular dynamics (BOMD) and the fast quantum mechanical molecular dynamics (Fast-QMMD) method with κ rescaled by 3/4 instead of 1/2.

TABLE II: Standard deviation, σ , of the total energy about its mean value and the upper bound of the systematic drift of the total energy, E_{drift} , computed from “exact” Born-Oppenheimer molecular dynamics (BOMD) and fast quantum mechanical molecular dynamics (Fast-QMMD) simulations of liquid isocyanic acid. The simulation were performed with the LATTE program in the non-orthogonal formulation, i.e. as implemented in Eqs. (50), (51) and (55) with the entropy term approximated by Eq. (56).

$k_B T_e$ (eV)		σ (μeV)	E_{drift} ($\mu\text{eV}/\text{atom}/\text{ps}$)
0.0	Fast-QMMD ($\tau = 0$)	0.315	5.10×10^{-3}
	Fast-QMMD ($\tau = 10^{-5}$)	0.702	0.285
	BOMD (4 SCF/step)	0.358	9.94×10^{-3}
0.5	Fast-QMMD (1/2) κ	2.47	1.43
	Fast-QMMD (3/4) κ	0.786	7.85×10^{-2}
	BOMD (4 SCF/step)	0.361	8.50×10^{-2}

terms of the convergence to “exact” Born-Oppenheimer molecular dynamics as a function of the finite integration time step δt . By comparing the deviation in forces, net Mulliken charges, and the total energy, between the fast quantum mechanical molecular dynamics scheme and an “exact” Born-Oppenheimer molecular dynamics as a function of δt we can study the consistency between the two methods. Figure 7 shows the difference between a fully converged “exact” Born-Oppenheimer molecular dynamics simulation and the fast quantum mechanical molecular dynamics scheme as measured by the root mean square deviation over 200 fs of simulation time. We find that the deviation of the nuclear forces, the charges $\{q_i\}$, as well as the total energy difference are of the or-

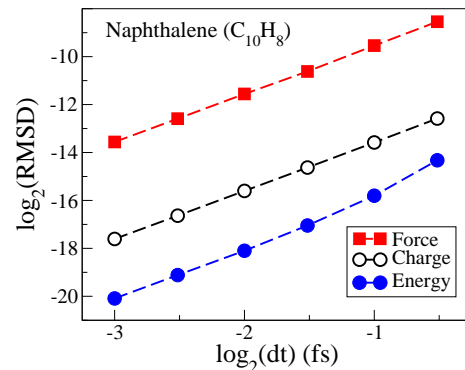


FIG. 7: The root mean square deviation (RMSD) between the fast quantum mechanical molecular dynamics, Eqs. (14)-(15), and “exact” (4 SCF/step) Born-Oppenheimer molecular dynamics, for the nuclear forces, the net Mulliken charges and the total energy for a Naphthalene molecule at room temperature. The simulation were performed with the LATTE molecular dynamics program using self-consistent-charge tight-binding theory in an orthogonal formulation at $T_e = 0$, i.e. as implemented in Eqs. (57), (58) and (60) with $S = 0$.

der δt^2 with a small pre-factor. This convergence demonstrates a consistency between the fast quantum mechanical scheme and Born-Oppenheimer molecular dynamics using Verlet integration, where the optimization-free scheme behaves as a well controlled and tunable approximation. As in “exact” Born-Oppenheimer molecular dynamics, the dominating error is governed by the local truncation error arising from the choice of finite integration time step δt , which is much larger than any difference between the fast quantum mechanical molecular dynamics and Born-Oppenheimer molecular dynamics.

V. SUMMARY AND CONCLUSIONS

Based on a free energy formulation of extended Lagrangian Born-Oppenheimer molecular dynamics in the limit of vanishing self-consistent-field optimization, we have derived and demonstrated a fast quantum mechanical molecular dynamics scheme, Eqs. (14) and (15), which with a high precision can match the accuracy and fidelity of Born-Oppenheimer molecular dynamics. In addition to the removal of the self-consistent-field optimization we have also demonstrated compatibility with low pre-factor linear scaling solvers. The combined scheme provides a very efficient, energy conserving, low-complexity method to perform accurate quantum molecular dynamics simulations. Our findings show how the computational gap between classical and quantum mechanical molecular dynamics simulations can be reduced significantly.

VI. ACKNOWLEDGMENT

We acknowledge support by the United States Department of Energy Office of Basic Energy Sciences and the LANL Laboratory Directed Research and Development Program. Discussions with E. Chisolm, J. Coe, T. Peery, S. Niklasson, C. Ticknor, C.J. Tymczak, and G. Zheng, as well as stimulating contributions at the T-Division Ten Bar Java group are gratefully acknowledged. LANL is operated by Los Alamos National Security, LLC, for the NNSA of the U.S. DOE under Contract No. DE-AC52-06NA25396.

VII. APPENDIX

A. Calculating the forces in Hartree-Fock theory

Here we present some details of the fast quantum mechanical molecular dynamics, Eqs. (14) and (15), using a simple but general Hartree-Fock formalism, which should be directly applicable to a broad class of hybrid and semi-empirical electronic structure schemes. Instead of the auxiliary density variable $n(\mathbf{r})$ we will here use the more general density matrix P . In this formalism the extended free-energy Lagrangian in Eq. (4) is given by

$$\begin{aligned} \mathcal{L}(\mathbf{R}, \dot{\mathbf{R}}; P, \dot{P}) &= \frac{1}{2} \sum_k M_k \dot{R}_k^2 - \mathcal{U}(\mathbf{R}; P) + T_e \mathcal{S}(\mathbf{R}; P) \\ &+ \frac{1}{2} \mu \text{Tr}[\dot{P}^2] - \frac{1}{2} \mu \omega^2 \text{Tr}[(\mathcal{D}_{\text{gs}} - P)^2], \end{aligned} \quad (17)$$

with the potential energy chosen as

$$\mathcal{U}(\mathbf{R}; P) = 2\text{Tr}[hD(P)] + \text{Tr}\{D(P)G[D(P)]\}, \quad (18)$$

and ground state (gs) density matrix \mathcal{D}_{gs} . $\mathcal{S}(\mathbf{R}; P)$ is an unspecified electronic entropy term, which will be determined by the requirement to make the derived forces variationally correct, and T_e is the electronic temperature. The Fockian (or the effective single-particle Hamiltonian) is

$$F[P] = h + G[P], \quad (19)$$

with the short-hand notation, $G[P] = 2J[P] - K[P]$, where $J[P]$ and $K[P]$ are the conventional Coulomb and exchange matrices, and h is the matrix of the one-electron part [5, 6]. The temperature dependent density matrix

$$D(P) = Z \left(e^{\beta(F^\perp[P] - \mu_0 I)} + 1 \right)^{-1} Z^T, \quad (20)$$

which corresponds to $\sigma[n]$ in Eq. (5), is given as a Fermi function of the orthogonalized Fockian,

$$F^\perp[P] = Z^T F[P] Z. \quad (21)$$

Here Z and its transpose Z^T are the inverse Löwdin or Cholesky-like factors of the overlap matrix, S , determined by the relation

$$Z^T S Z = I. \quad (22)$$

At zero electronic temperature ($T_e = 0$ K) the Fermi-operator expansion in Eq. (20) is given by the Heaviside step function, with the step formed at the chemical potential μ_0 , separating the occupied from the unoccupied states.

The Euler-Lagrange equations of motion of \mathcal{L} in Eq. (17) are given by

$$\begin{aligned} M_k \ddot{R}_k &= - \left. \frac{\partial \mathcal{U}}{\partial R_k} \right|_P + T_e \left. \frac{\partial \mathcal{S}}{\partial R_k} \right|_P \\ &- \frac{1}{2} \mu \omega^2 \left. \frac{\partial}{\partial R_k} \text{Tr}[(\mathcal{D}_{\text{gs}} - P)^2] \right|_P, \end{aligned} \quad (23)$$

and

$$\mu \ddot{P} = \mu \omega^2 (\mathcal{D}_{\text{gs}} - P) - \left. \frac{\partial \mathcal{U}}{\partial P} \right|_{\mathbf{R}} + T_e \left. \frac{\partial \mathcal{S}}{\partial P} \right|_{\mathbf{R}}. \quad (24)$$

A cumbersome but fairly straightforward derivation (see Ref. [42] for a closely related example), using the relation and notation $Z_{R_k} = \partial Z / \partial R_k = -(1/2) S^{-1} S_{R_k} Z$, and defining the \mathcal{S} term such that

$$T_e \left. \frac{\partial \mathcal{S}}{\partial P_{ij}} \right|_{\mathbf{R}} = 2\text{Tr} \left[F^\perp [D] D_{P_{ij}}^\perp \right] \quad (25)$$

and

$$T_e \left. \frac{\partial \mathcal{S}}{\partial R_k} \right|_P = 2\text{Tr} \left[F^\perp [D] D_{R_k}^\perp \right], \quad (26)$$

gives the equations of motion

$$\begin{aligned} M_k \ddot{R}_k &= -2\text{Tr}[h_{R_k} D] - \text{Tr}[DG_{R_k}(D)] \\ &+ \text{Tr}[(DF[D]S^{-1} + S^{-1}F[D]D)S_{R_k}] \\ &- \frac{1}{2} \mu \omega^2 \left. \frac{\partial}{\partial R_k} \text{Tr}[(\mathcal{D}_{\text{gs}} - P)^2] \right|_P, \end{aligned} \quad (27)$$

and

$$\mu \ddot{P} = \mu \omega^2 (\mathcal{D}_{\text{gs}} - P). \quad (28)$$

Notice that because of matrix symmetry P_{ij} is not independent from P_{ji} . The partial derivatives of matrix elements P_{ij} are therefore both over P_{ij} and P_{ji} . In the limit $\mu \rightarrow 0$, we get the final equations of motion for the fast quantum mechanical molecular dynamics scheme,

$$\begin{aligned} M_k \ddot{R}_k &= -2\text{Tr}[h_{R_k} D] - \text{Tr}[DG_{R_k}(D)] \\ &+ \text{Tr}[(DF[D]S^{-1} + S^{-1}F[D]D)S_{R_k}], \end{aligned} \quad (29)$$

$$\ddot{P} = \omega^2 (D(P) - P), \quad (30)$$

where we have included the substitution of \mathcal{D}_{gs} with $D(P)$ in the same way as in Eq. (15), i.e. with ω^2 rescaled by a constant $c \leq 1$. The notation for the

partial derivative of the two-electron term is defined as $G_{R_k}(D) = \partial G(D)/\partial R_k|_D$, i.e. under the condition of constant density matrix D .

The last term in Eq. (29), which includes the basis-set dependence S_{R_k} is the Pulay force term that here is given in a generalized form that is valid also for non-idempotent density matrices at finite electronic temperatures [42].

B. Approximate Entropy contribution

The $\mathcal{S}[\mathbf{R}; P]$ term is defined such that the two conditions in Eqs. (25) and (26) are fulfilled. At the self-consistent ground state density, i.e. when $P = D = \mathcal{D}_{\text{gs}}$, both these conditions are automatically satisfied by the corresponding regular ground state (gs) electronic entropy contribution to the free energy [9],

$$\begin{aligned} \mathcal{S}_{\text{gs}}[\mathbf{R}; P] &= \mathcal{S}_{\text{gs}}[\mathbf{R}; D^\perp(P)] \\ &= -2k_B \text{Tr}[D^\perp \ln(D^\perp) + (I - D^\perp) \ln(I - D^\perp)], \end{aligned} \quad (31)$$

where the relation between D^\perp and D is given by the congruence transformation

$$D = ZD^\perp Z^T. \quad (32)$$

A related derivation is given in Ref. [42]. Using the approximate estimate $\mathcal{S}_{\text{gs}}[\mathbf{R}; P]$ in Eq. (31) when P and D deviate from the ground state gives,

$$\begin{aligned} T_e \left. \frac{\partial \mathcal{S}}{\partial P_{ij}} \right|_{\mathbf{R}} &= 2\text{Tr} \left[F^\perp[P] D_{P_{ij}}^\perp \right], \\ T_e \left. \frac{\partial \mathcal{S}}{\partial R_k} \right|_P &= 2\text{Tr} \left[F^\perp[P] D_{R_k}^\perp \right], \end{aligned} \quad (33)$$

which only approximately fulfills the conditions in Eqs. (25) and (26). It is possible to show that the error is linear in $\delta P = D - P$ by a linearization of $F^\perp[D]$ around P . Since $D(P)$ and P can be assumed to be close to the ground state, δP is small. From the scaling result illustrated in Fig. 7 the error should therefore be quadratic in the integration time step, i.e. $\sim \delta t^2$. We may therefore approximate the total free energy using $\mathcal{S}_{\text{gs}}[\mathbf{R}; P]$, which is zero at $T_e = 0$ K. However, for the exact formulation and derivation of the equations of motion, Eqs. (29) and (30), the entropy contribution, $T_e \mathcal{S}[\mathbf{R}; P]$, is unknown, both at finite and zero temperatures. As is seen in the equations of motion, Eqs. (29) and (30), this does not affect the forces or the dynamics, only the estimate of the constant of motion,

$$E_{\text{tot}} = \frac{1}{2} \sum_k M_k \dot{R}_k^2 + \mathcal{U}[\mathbf{R}; P] - T_e \mathcal{S}[\mathbf{R}; P], \quad (34)$$

is approximated. By comparing the approximate E_{tot} to optimized ‘‘exact’’ Born-Oppenheimer molecular dynamics simulations, the accuracy of the dynamics can be estimated.

C. Alternative potential energy forms

As an alternative to the potential energy, $\mathcal{U}(\mathbf{R}; P)$, in Eq. (18) we may choose other functional forms that are equivalent at the ground state, i.e. when $P = D = \mathcal{D}_{\text{gs}}$. By using the Harris-Foulkes-like relation [33, 34],

$$\text{Tr}[DG(D)] \approx \text{Tr}[(2D - P)G(P)], \quad (35)$$

which has an error of second order in $\delta P = D - P$, we may, for example, choose

$$\mathcal{U}[\mathbf{R}; P] = 2\text{Tr}[hD(P)] + \text{Tr}\{[2D(P) - P]G(P)\}, \quad (36)$$

as our potential energy term. In this case, the equations of motion at $T_e = 0$ corresponding to Eqs. (29) and (30) become

$$\begin{aligned} M_k \ddot{R}_k &= -2\text{Tr} [h_{R_k} D] - \text{Tr}\{[2D - P]G_{R_k}(P)\} \\ &+ \text{Tr} [(DF[P]S^{-1} + S^{-1}F[P]D)S_{R_k}], \end{aligned} \quad (37)$$

and

$$\ddot{P} = \omega^2 (D - P), \quad (38)$$

with the constant of motion

$$E_{\text{tot}} = \frac{1}{2} \sum_k M_k \dot{R}_k^2 + 2\text{Tr}[hD] \quad (39)$$

$$+ \text{Tr}\{(2D - P)G(P)\} - T_e \mathcal{S}(\mathbf{R}; P).$$

The entropy term that makes the nuclear forces variationally correct is here fulfilled by the expression in Eq. (31). With this choice of potential our dynamics only requires one Fockian or effective single particle Hamiltonian construction per time step. Unfortunately, the error in the Pulay force has been found to be large compared to Eq. (29). The dynamics in Eqs. (37) and (38) should therefore be used only for orthogonal representations, i.e. when the overlap matrix $S = I$.

D. Self-Consistent-Charge Density Functional Tight-Binding Theory

In self-consistent-charge density functional based tight-binding theory [47–50] the continuous electronic density, $\sigma(\mathbf{n})$, or the density matrix, $D(P)$, in Eq. (18) is replaced by the net Mulliken charges $\mathbf{q}[\mathbf{n}] = \{q_i\}$ for each atom i , where $\mathbf{n} = \{n_i\}$ are the dynamical variables corresponding to P . The potential energy functional \mathcal{U} in Eq. (18) is then reduced to

$$\mathcal{U}[\mathbf{R}; \mathbf{n}] = 2 \sum_{i \in \text{occ}} \varepsilon_i - \frac{1}{2} \sum_{i,j} q_i(\mathbf{n}) q_j(\mathbf{n}) \gamma_{ij} + E_{\text{pair}}[\mathbf{R}]. \quad (40)$$

Here ε_i are the (doubly) occupied eigenvalues of the charge dependent effective single-particle Hamiltonian

$$\begin{aligned} H_{i\alpha,j\beta}[\mathbf{n}] &= h_{i\alpha,j\beta} \\ &+ (1/2) \sum_{k\beta'} (S_{i\alpha,k\beta'} V_{k\beta',j\beta}^{ee} + V_{i\alpha,k\beta'}^{ee} S_{k\beta',j\beta}) \end{aligned} \quad (41)$$

where

$$V_{j\beta,k\beta'}^{ee} = \sum_l q_l(\mathbf{n}) \gamma_{jl} \delta_{jk} \delta_{\beta'\beta}, \quad (42)$$

$h_{i\alpha,j\beta}$ is a parameterized Slater-Koster tight-binding Hamiltonian, $S_{i\alpha,j\beta}$ the overlap matrix, i and j are atomic indices and α and β are orbital labels [51]. The net Mulliken charges are given by

$$q_i[\mathbf{n}] = 2 \sum_{\alpha \in i} \left(\varrho_{i\alpha,i\alpha}^\perp - \varrho_{i\alpha,i\alpha}^{0\perp} \right), \quad (43)$$

with the density matrix

$$\varrho^\perp = \varrho^\perp[\mathbf{n}] = \left(e^{\beta(H^\perp[\mathbf{n}] - \mu_0 I)} + 1 \right)^{-1}, \quad (44)$$

using the orthogonalized Hamiltonian

$$H^\perp[\mathbf{n}] = Z^T H[\mathbf{n}] Z. \quad (45)$$

Here ϱ^0 is the density matrix of the corresponding separate non-interacting atoms. The de-orthogonalized density matrix is

$$\varrho = \varrho[\mathbf{n}] = Z \varrho^\perp[\mathbf{n}] Z^T, \quad (46)$$

and as above, the congruence transformation factors are defined through

$$Z^T S Z = I, \quad (47)$$

where S is the basis set overlap matrix.

The electron-electron interaction in Eq. (40) is determined by γ_{ij} , which decays like $1/R$ at large distances and equals the Hubbard repulsion for the on-site interaction. $E_{\text{pair}}[\mathbf{R}]$ is a sum of pair potentials, $\phi(R)$, that provide short-range repulsion. The radial dependence, $\zeta(R)$, of the Slater-Koster bond integrals, elements of the overlap matrix, and the $\phi(R)$ are all represented analytically in LATTE by the mathematically convenient form,

$$\zeta(R) = A_0 \prod_{i=1}^4 \exp(A_i R^i), \quad (48)$$

where A_0 to A_4 are adjustable parameters that are fitted to the results of quantum chemical calculations on small molecules. To ensure that the off-diagonal elements of h and S and the $\phi(R)$ in our self-consistent tight-binding implementation decay smoothly to zero at a specified distance, R_{cut} , we replace the $\zeta(R)$ by cut-off tails of the form,

$$t(R) = B_0 + \Delta R(B_1 + \Delta R(B_2 + \Delta R(B_3 + \Delta R(B_4 + \Delta R B_5)))) \quad (49)$$

at $R = R_1$, where $\Delta R = R - R_1$ and B_0 to B_5 are adjustable parameters. The adjustable parameters are parameterized to match the value and first and second derivatives of $t(R)$ and $\zeta(R)$ at $R = R_1$ and to set the value and first and second derivatives of $t(R)$ to zero at $R = R_{\text{cut}}$.

1. Non-orthogonal representation at $T_e \geq 0$

The fast quantum mechanical molecular dynamics scheme, Eqs. (29) and (30) or Eqs. (8) and (9), using self-consistent tight-binding theory in its non-orthogonal formulation is given by

$$\begin{aligned} M_k \ddot{R}_k &= -2Tr[\varrho H_{R_k}] \\ &+ \frac{1}{2} \sum_{i,j} q_i q_j \frac{\partial \gamma_{ij}}{\partial R_k} + \sum_{i,j} q_i \gamma_{ij} \frac{\partial q_j}{\partial R_k} \Big|_\varrho \\ &+ Tr[(S^{-1} H[\mathbf{q}] \varrho + \varrho H[\mathbf{q}] S^{-1}) S_{R_k}] - \frac{\partial E_{\text{pair}}[\mathbf{R}]}{\partial R_k}, \end{aligned} \quad (50)$$

and

$$\ddot{n}_i = \omega^2 (q_i - n_i), \quad (51)$$

where

$$H_{R_k} = \frac{\partial H}{\partial R_k} \Big|_\varrho \quad (52)$$

and

$$S_{R_k} = \frac{\partial S}{\partial R_k}. \quad (53)$$

The partial derivatives of q_j and H in Eqs. (50) and (52) are with respect to a constant density matrix ϱ in its non-orthogonal form, i.e. including an S dependence of q_j ,

$$\frac{\partial q_j}{\partial R_k} \Big|_\varrho = 2 \sum_{\alpha \in j} (\varrho S_{R_k})_{j\alpha, j\alpha}. \quad (54)$$

The total energy is given by

$$\begin{aligned} E_{\text{tot}} &= \frac{1}{2} \sum_k M_k \dot{R}_k^2 + 2 \sum_{i \in \text{occ}} \varepsilon_i \\ &- \frac{1}{2} \sum_{i,j} q_i q_j \gamma_{ij} + E_{\text{pair}}[\mathbf{R}] - T_e \mathcal{S}[\mathbf{R}; \mathbf{n}], \end{aligned} \quad (55)$$

with the entropy contribution to the free energy approximated by

$$\mathcal{S}[\mathbf{R}; \mathbf{n}] \approx -2k_B \sum_i \{f_i \ln(f_i) + (1 - f_i) \ln(1 - f_i)\}. \quad (56)$$

Here $f_i = f_i[n]$ are the eigenstates of the Fermi operator expansion $\varrho^\perp[n]$ of $H^\perp[\mathbf{n}]$ in Eq. (44).

2. Orthogonal representation at $T_e = 0$

For orthogonal formulations, i.e. when $S = I$, and at zero electronic temperature, $T_e = 0$, we will base our

dynamics on the equations of motion in Eqs. (37) and (38). In this case the fast quantum mechanical molecular dynamics scheme, Eqs. (50)-(51), is given by

$$M_k \ddot{\mathbf{R}}_k = -2Tr[\rho H_{R_k}] + \frac{1}{2} \sum_{i,j} \left(n_i n_j \frac{\partial \gamma_{ij}}{\partial R_k} \right) - \frac{\partial E_{\text{pair}}[\mathbf{R}]}{\partial R_k}, \quad (57)$$

$$\ddot{n}_i = \omega^2 (q_i - n_i), \quad (58)$$

where

$$\{H_{R_k}[\mathbf{n}]\}_{i\alpha,j\beta} = \frac{\partial h_{i\alpha,j\beta}}{\partial R_k} + \sum_l n_l \frac{\partial \gamma_{il}}{\partial R_k} \delta_{ij} \delta_{\alpha\beta}. \quad (59)$$

The density matrix is given directly from the step function of the Hamiltonian, $\rho = \theta(\mu_0 I - H[\mathbf{n}])$, without any de-orthogonalization that requires the calculation of the inverse factorization of the overlap matrix, Eq. (47). The constant of motion, E_{tot} , is approximate by

$$E_{\text{tot}} = \frac{1}{2} \sum_k M_k \dot{\mathbf{R}}_k^2 + 2 \sum_{i \in \text{occ}} \varepsilon_i - \frac{1}{2} \sum_{i,j} (2n_i - q_i) n_j \gamma_{ij} + E_{\text{pair}}[\mathbf{R}]. \quad (60)$$

3. General remarks

Apart from the first few initial molecular dynamics time steps, where we apply a high degree of self-consistent-field convergence and set $\mathbf{n} = \mathbf{q}$, no ground state self-consistent-field optimization is required. The density matrix, ρ , and the Hamiltonian, H , necessary in the force calculations (and for the total energy) are calculated only once per time step in the orthogonal case with one additional construction of the Hamiltonian required in non-orthogonal simulations. The numerical integration of the equations of motion in Eq. (14) is performed with the velocity Verlet scheme and in Eq. (15) with the modified Verlet scheme in Eq. (16) as described in Ref. [36]. For the examples presented here we used the modified Verlet scheme including dissipation ($\alpha > 0$) with $K = 5$ and the constant $\kappa = \delta t^2 \omega^2$ as given in Ref. [36] was rescaled by a factor 1/2 in all examples except for one of the test cases in Fig. 6.

-
- [1] M. Karplus and J. A. McCammon, *Nat. Struct. Biol.* **9**, 646 (2002).
 - [2] D. Marx and J. Hutter, *Modern Methods and Algorithms of Quantum Chemistry* (ed. J. Grotendorst, John von Neumann Institute for Computing, Jülich, Germany, 2000), 2nd ed.
 - [3] I. S. Y. Wang and M. Karplus, *J. Am. Chem. Soc.* **95**, 8160 (1973).
 - [4] C. Leforestier, *J. Chem. Phys.* **68**, 4406 (1978).
 - [5] C. C. J. Roothaan, *Rev. Mod. Phys.* **23**, 69 (1951).
 - [6] R. McWeeny, *Rev. Mod. Phys.* **32**, 335 (1960).
 - [7] P. Hohenberg and W. Kohn, *Phys. Rev.* **136**, B:864 (1964).
 - [8] W. Kohn and L. J. Sham, *Phys. Rev. B* **140**, A1133 (1965).
 - [9] R. G. Parr and W. Yang, *Density-functional theory of atoms and molecules* (Oxford University Press, Oxford, 1989).
 - [10] R. M. Dreizler and K. U. Gross, *Density-functional theory* (Springer Verlag, Berlin Heidelberg, 1990).
 - [11] R. P. Feynman, *Phys. Rev.* **56**, 367 (1939).
 - [12] P. Pulay and G. Fogarasi, *Chem. Phys. Lett.* **386**, 272 (2004).
 - [13] A. M. N. Niklasson, C. J. Tymczak, and M. Challacombe, *Phys. Rev. Lett.* **97**, 123001 (2006).
 - [14] T. D. Kühne, M. Krack, F. R. Mohamed, and M. Parrinello, *Phys. Rev. Lett.* **98**, 066401 (2006).
 - [15] P. Ehrenfest, *Z. Phys.* **45**, 455 (1927).
 - [16] J. L. Alonso, X. Andrade, P. Echenique, F. Falceto, D. Prada-Garcia, A. Rubio, *Phys. Rev. Lett.* **101**, 096403 (2008).
 - [17] J. Jakowski, and K. Morokuma, *J. Chem. Phys.* **130**, 224106 (2009).
 - [18] R. Car and M. Parrinello, *Phys. Rev. Lett.* **55**, 2471 (1985).
 - [19] M. Tuckerman, *J. Phys.:Condens. Matter* **50**, 1297 (2002).
 - [20] B. Hartke, and E. A. Carter, *Chem. Phys. Lett.* **189**, 358 (1992).
 - [21] H. B. Schlegel, J. M. Millam, S. S. Iyengar, G. A. Voth, A. D. Daniels, G. Scuseria, and M. J. Frisch, *J. Chem. Phys.* **114**, 9758 (2001).
 - [22] J. Herbert, and M. Head-Gordon, *J. Chem. Phys.* **121**, 11542 (2004).
 - [23] B. Kirchner J. di Dio Philipp, and J. Hutter, *Top. Curr. Chem.* **307**, 109 Springer Verlag, Berlin Heidelberg, (2012).
 - [24] S. Goedecker, *Rev. Mod. Phys.* **71**, 1085 (1999).
 - [25] D. R. Bowler and T. Miyazaki, *Rep. Prog. Phys.* **75**, 036503 (2012).
 - [26] A. M. N. Niklasson, *Phys. Rev. B* **66**, 155115 (2002).
 - [27] M. J. Cawkwell and A. M. N. Niklasson, *J. Chem. Phys.* (accepted for publication).
 - [28] A. M. N. Niklasson, *Phys. Rev. B* **68**, 233104 (2003).
 - [29] F. Mauri, and G. Galli, *Phys. Rev. B* **50**, 4316 (1994).
 - [30] A. P. Horsfield, A. M. Bratkovsky, M. Fern, D. G. Pettifor, and M. Aoki, *Phys. Rev. B* **54**, 12694 (1996).
 - [31] E. Tushida, *J. Phys.: Condens. Matter* **20**, 294212 (2008).
 - [32] F. Shimojo, R. K. Kalia, A. Nakono, and P. Vashista, *Phys. Rev. B* **77**, 085103 (2008).
 - [33] J. Harris, *Phys. Rev. B* **31**, 1770 (1985).
 - [34] W. M. C. Foulkes and R. Haydock, *Phys. Rev. B* **39**,

- 12520 (1989).
- [35] A. M. N. Niklasson, Phys. Rev. Lett. **100**, 123004 (2008).
- [36] A. M. N. Niklasson, P. Steneteg, A. Odell, N. Bock, M. Challacombe, C. J. Tymczak, E. Holmström, G. Zheng, and V. Weber, J. Chem. Phys. **130**, 214109 (2009).
- [37] P. Steneteg, I. A. Abrikosov, V. Weber, and A. M. N. Niklasson, Phys. Rev. B **82**, 075110 (2010).
- [38] G. Zheng, A. M. N. Niklasson, and M. Karplus, J. Chem. Phys. **135**, 044122 (2011).
- [39] A. M. N. Niklasson, P. Steneteg, and N. Bock, J. Chem. Phys. **135**, 164111 (2011).
- [40] M. Weinert and J. W. Davenport, Phys. Rev. B **45**, R13709 (1992).
- [41] R. M. Wentzcovitch, J. L. Martins, and P. B. Allen, Phys. Rev. B **45**, R11372 (1992).
- [42] A. M. N. Niklasson, J. Chem. Phys. **129**, 244107 (2008).
- [43] P. H. Dederichs and R. Zeller, Phys. Rev. B **28**, 5262 (1983).
- [44] B. Leimkuhler and S. Reich, *Simulating Hamiltonian Dynamics* (Cambridge University Press, 2004).
- [45] A. Odell, A. Delin, B. Johansson, N. Bock, M. Challacombe, and A. M. N. Niklasson, **131**, 244106 (2009), J. Chem. Phys.
- [46] A. Odell, A. Delin, B. Johansson, M. Cawkwell, and A. M. N. Niklasson, **135**, 224105 (2011), J. Chem. Phys.
- [47] A. P. Sutton, M. W. Finnis, D. G. Pettifor, and Y. Ohta, J. Phys. C: Solid State Phys. **21**, 35 (1988).
- [48] M. W. Finnis, A. T. Paxton, M. Methfessel, and M. van Schilfgaarde, Phys. Rev. Lett. **81**, 5149 (1998).
- [49] M. Elstner, D. Poresag, G. Jungnickel, J. Elstner, M. Haugk, T. Frauenheim, S. Suhai, and G. Seifert, Phys. Rev. B **58**, 7260 (1998).
- [50] M. Finnis, *Interatomic forces in condensed matter* (Oxford University Press, 2003).
- [51] E. Sanville, N. Bock, W. M. Challacombe, A. M. N. Niklasson, M. J. Cawkwell, D. M. Dattelbaum, and S. Sheffield, *Proceedings of the Fourteenth International Detonation Symposium* (Office of Naval Research, Arlington VA, ONR-351-10-185, 2010), pp. 91–101.
- [52] E. H. Rubensson and E. Rudberg, J. Phys.: Condes. Matter **23**, 075502 (2011).